

COURSE CONTENT FOR TRANSIT TRAINING

1 Implementation of a Wide Area Monitoring System

1.1 Introduction

The electric power system is a critical infrastructure, with faults or failures significantly impacting industrial production, business operations, and human safety. The rising demand for electricity and the competitive deregulated market have pushed utilities to operate power systems near their physical limits, making them susceptible to contingencies caused by severe faults. Ensuring fault-free operation and continuous electricity supply requires accurate, reliable, and near real-time monitoring and protection schemes to prevent fault propagation. Contemporary Supervisory Control and Data Acquisition (SCADA) systems, however, exhibit limitations in meeting these requirements.

In particular SCADA systems that are typically housed in power system control centers, monitor and control power system operations. They include applications for contingency analysis, voltage stability analysis, optimal power flow, economic dispatch, load forecasting, and bad data detection. Central to SCADA systems is the state estimator, which provides power system operating conditions at regular intervals based on raw measurements from substations and network topology. For accurate state estimation, observability analysis is conducted before each state estimation execution.

One significant weakness of SCADA systems is their slow response time, which compromises quasi real-time monitoring and control. SCADA measurements are sequentially received from Remote Terminal Units (RTUs) at intervals of 2-10 seconds, causing delays that can allow contingencies to propagate. This slow reporting rate stems from the asynchronous polling of RTUs and the time required to scan all RTUs, particularly in large power systems [1].

The assumption of a static power system, due to its large inertia, once justified these delays. However, the increasing penetration of renewable energy sources, driven by low CO₂ emission goals and financial incentives, challenges this assumption. Renewable energy sources introduce unpredictable energy production and fast-operating power electronic devices, necessitating faster and more accurate measurement technologies than those provided by conventional SCADA systems.

The advent of Synchronized Measurement Technology (SMT) in the early 1980s, specifically the development of Phasor Measurement Units (PMUs), marked a significant advancement in power system monitoring and control [1]. PMUs offer high-accuracy, high-speed measurements of voltage and current phasors, synchronized across different locations via GPS signals, enabling precise phase comparisons. PMUs provide time-stamped measurements with high accuracy, supporting real-time and synchronized monitoring. The fast reporting rate (up to 50 phasors per second in a 50 Hz system) and precise angle measurements of PMUs represent significant improvements over conventional measurement devices.

To ensure interoperability and performance consistency among PMUs from different vendors, IEEE established several standards, including:

- IEEE 1344-1995: The original synchrophasor standard [2].
- IEEE C37.118-2005: Updated standard addressing synchronization, time tags, measurement compliance, and communication formats [3].
- IEEE C37.118.1-2011 and C37.118.2-2011: Separated measurement and communication standards [4].
- IEEE C37.118.1a-2014: Amended performance requirements for PMUs [5].

Compliance with these standards is crucial for effective wide area monitoring systems. Exploiting PMU features and applying SMT to power system measurement layer initiates a new era in power system monitoring and control. The high fidelity and real-time reporting capabilities of PMUs enhance the visualization of power system conditions. SMT facilitates the transition from traditional SCADA systems to advanced Wide Area Monitoring (WAM) systems. These systems incorporate existing and new applications based on synchronized phasor measurements, improving performance and enabling more effective monitoring and control of power systems [6].

The integration of PMUs and SMT into power systems represents a pivotal advancement, addressing the limitations of conventional SCADA systems and supporting the development of robust WAM systems. This transition enhances situational awareness, reliability, and the ability to manage the dynamic challenges of modern power systems.

1.2 Infrastructure Implementation of a Wide Area Monitoring System

1.2.1 Overview

Wide Area Monitoring (WAM) systems are critical for modern power grids, providing enhanced situational awareness and operational efficiency. These systems utilize advanced technologies such as SMT to collect synchronized data across large geographical areas, enabling real-time monitoring and control. The cornerstone of WAM systems is the Phasor Measurement Unit (PMU), a device that measures electrical signals on an electricity grid to determine the magnitude and phase angle of the voltage and current sine waves. PMUs offer a high reporting rate of 50 times per second, compared to the 2-5 second intervals of traditional systems. GPS synchronization ensures that all measurements are time-synchronized, providing a coherent picture of the grid's status. Additionally, except of voltage and current, PMUs are capable of measuring frequency and the rate of change of frequency (ROCOF).

The benefits from the application of a WAM system are numerous for the effective operation of the power grid. The power system operators are able to have a wide area visualization of the power system operating condition in real time with enhanced accuracy. In this context, the KIOS Center of Excellence of the University of Cyprus in collaboration with the Cyprus Transmission System Operator and the Electricity Authority of Cyprus have implemented a WAM System that renders the

transmission level of the Cyprus power system completely observable by the PMU measurements. In this training session, useful insights and experiences are provided for the successful implementation of a WAM system. Further, insights for three different WAM-based applications are discussed in this training material to show the applicability of research oriented applications in the real field.

1.2.2 Design of the measuring infrastructure of the WAM system

The measurement infrastructure forms the backbone of a WAM system. Therefore, it is crucial to design this infrastructure effectively to support the needs of all the tools and applications developed within the WAM system. To achieve a fully PMU-observable power system, the design of the measurement infrastructure will need to be developed almost from scratch. This involves selecting PMUs that meet the technical requirements of the project and determining the substations where these PMUs will be installed. This section will first provide a detailed description of the selection criteria for the PMU to be selected. Following this, the methodology for selecting optimal PMU locations to ensure the power system is fully observable while minimizing the number of PMUs will be presented.

1.2.2.1 *Selection of the PMU*

To achieve a PMU-observable power system in a cost-effective manner for the EMPOWER project, it is essential to select PMUs that are both scalable and economically feasible. Full system observability requires monitoring all lines connected to each substation, measuring the currents flowing through them with the installed PMU. However, because substations vary in the number of lines they have, a PMU with a fixed number of measuring channels would lack the necessary adaptability. If a PMU has more channels than needed, some would go unused, wasting resources. Conversely, if there are more lines than channels, multiple PMUs would be required per substation, significantly increasing infrastructure costs. Thus, adaptability to different substation configurations is a key criterion in selecting the appropriate PMU.

One solution for this requirement is the SEL-2240 Axion PMU, offered by Schweitzer Engineering Laboratories and shown in *Figure 1*. This PMU provides the flexibility to configure its measuring channels to match the number of lines at a substation. This PMU is a comprehensive, modular solution for digital I/O, analog input, current and voltage measurement, and control, suitable for various utility and industrial applications. Therefore, that was the PMU that was used in several substations in the implementation of the WAM in the Cyprus power system.



Figure 1: SEL 2240-Axion PMU

1.2.2.2 Determination of the PMU locations in the power system

One of the primary objectives in the implementation of a WAM system is to achieve full observability through the use of PMU measurements. To accomplish this, it is essential to determine the minimum number of PMUs needed for complete system observability. To address this challenge, a graph-based method can be deployed to identify the optimal PMU locations.

The methodology employs binary integer linear programming to find the optimal combination of substations, ensuring the installation of the fewest possible PMUs. Within this programming framework, various constraints can be applied, such as excluding substations from PMU installation due to the absence of necessary communication or measurement infrastructure.

In order to obtain the optimal PMU locations through the binary integer linear programming the objective function can be defined as,

$$\begin{aligned} \min \mathbf{c}^T \mathbf{X} \\ \text{s. t. } \mathbf{A}\mathbf{X} \geq \mathbf{b} \\ \mathbf{l}_b \leq \mathbf{X} \leq \mathbf{u}_b \end{aligned} \quad (1)$$

Where \mathbf{X} is a binary decision variable vector, defined as

$$x_i = \begin{cases} 1 & \text{if a PMU is placed at bus } i \\ 0 & \text{otherwise} \end{cases}, \quad (2)$$

The topology of the system in a graph representation should be available and used as input to the optimal PMU location problem. For this purpose, a binary connectivity matrix \mathbf{A} for the power system is formulated as,

$$A(i, j) = \begin{cases} 1 & \text{if } i = j \\ 1 & \text{if bus } i \text{ and } j \text{ are connected} \\ 0 & \text{otherwise} \end{cases} \quad (3)$$

The vector c contains the cost coefficients of the PMUs. In the case that all PMUs that will be installed in the power system have the same cost this vector can be unity. The goal is to ensure that every bus (substation) in the power system is observable, either directly by having a PMU installed on it or indirectly by being connected to a bus with a PMU. Thus, the vector b in constraint (1) must always be equal to or greater than one to guarantee full observability by PMUs.

The second constraint in (1) addresses specific cases where a PMU cannot be installed at a particular bus. This is done by setting the corresponding element in the upper bound (ub) vector to 0. Conversely, if a PMU must be installed at a specific bus, the corresponding element in the lower bound (lb) vector is set to 1. This constraint accounts for infrastructure limitations at certain substations where PMU installation is not feasible or where the criticality of the substation necessitates PMU installation.

To solve the optimization problem outlined in (1) for a power system, a binary connectivity matrix of the buses should be first formulated based on the network topology provided. The optimization problem can be solved through open source solvers or using Matlab software, and the solution indicates the number and the locations of the PMUs to achieve full system observability.

1.2.3 Design of the Communication Infrastructure

The success of a real-time wide-area monitoring and control system is critically dependent on the communication infrastructure that enables the transfer of measurements from the field to the power system control center. Key aspects of this communication infrastructure include the selection of appropriate communication protocols, managing data transfer volumes, ensuring data quality, and minimizing data latency. Each of these factors must be considered to ensure that measurements are transmitted to the control center both promptly and reliably. Any deviation from the required standards in these areas can compromise the effectiveness of real-time applications that depend on PMU measurements. Thus, the design of the communication infrastructure must prioritize these considerations to support the functionality and integrity of the monitoring and control system.

1.2.3.1 *Communication architecture and communication medium*

A typical multi-layered architecture for transferring PMU measurements to the Control Center is illustrated in *Figure 2*. The first layer consists primarily of PMUs installed at various power system substations. In the second layer, Phasor Data Concentrators (PDCs) collect and time-align the measurements from these PMUs. The PDCs then forward the synchronized data to the Control Center, where it is utilized by applications for monitoring and controlling power system operations.

The physical layer of the communication network significantly influences the overall performance of the wide-area monitoring and control system. A key decision in designing the communication infrastructure is choosing between two distinct approaches: using the existing Internet network as the foundation for the intra-power network or developing a dedicated, scalable communication network specifically for the power infrastructure.

In the case of the WAM system implemented in Cyprus, the Electricity Authority of Cyprus operates a private communication network. Therefore, it was decided to transmit PMU measurements through this private network to mitigate potential data quality issues. The EAC's telecommunication network has a lower incidence of data dropouts compared to public networks and offers enhanced

protection against cyberattacks due to its privacy, ensuring more secure and reliable transmission of PMU data.

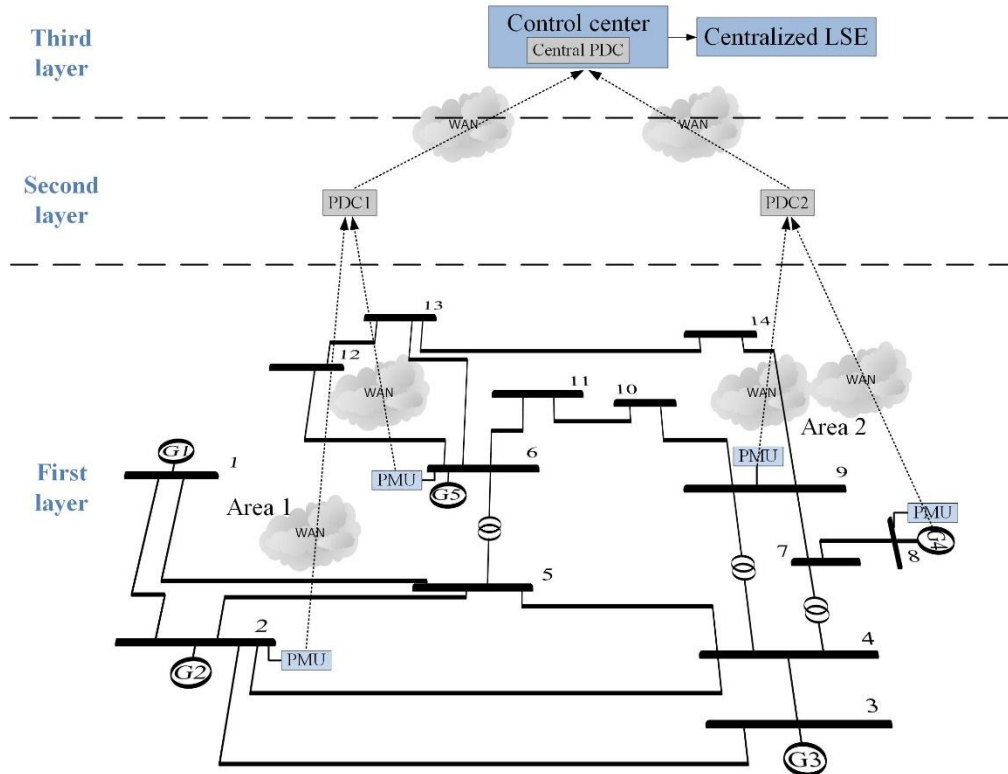


Figure 2: Multi-layered PMU architecture

One of the key advantages of WAM systems over traditional SCADA systems is their ability to respond to power oscillations, voltage fluctuations, and frequency instability in real-time or near-real-time. To effectively manage these issues, it is crucial to acquire real-time data from the power field with minimal delay, as certain contingencies need to be addressed within milliseconds of their occurrence.

Several factors contribute to data delay in a WAM system before the data reaches the control center. These include delays from transducers, which measure the RMS current and voltage of the busbars; the window size of the Discrete Fourier Transform used by PMUs to digitize analog voltage and current signals; the time required for phasor calculation; the size of the PMU data output; the alignment of phasors in the PDCs; and the latency associated with the communication link.

While many of these delays are inherent to the hardware devices and thus unavoidable, the communication link's delay can be minimized by selecting a link with the lowest data transfer latency.

Table 1 provides a comparison of various communication links currently used in networks, along with their associated delays in a WAM communication network. According to the table, fiber optic and digital microwave links offer the lowest data latency compared to other data transfer mediums.

Table 1: Associated delay of different communication links

Communication link	Approximated delay-one way (ms)
Fiber-optic cable	100-150
Digital microwave link	100-150
Power line	150-350
Telephone line	200-300
Satellite link	500-700

1.3 Wide Area Monitoring Applications

The implementation of the measuring and communication infrastructure of the WAM system consists of the first critical milestone for realizing a WAM system. The high quality, rich PMU data that are received at the control center should be processed in an automatic way by different monitoring applications and provide critical information to the power system control center in real time. Thus, implementation of PMU-based applications that can be accommodated in a WAM system is the next critical milestone for realizing a WAM system. This Section provides the insights for 3 PMU-based applications namely the state estimation, line parameter estimation, and inertia estimation.

1.3.1 Real time state estimation

In a power system that is fully observable by PMUs, some states of the system will be direct measurements from PMUs, and the remaining will be estimated or derived by using the directly measured voltage phasors and current phasors, assuming known transmission line parameters [7]. A dynamic SE can then be used to estimate the most likely voltage phasors for all the buses in the system in real time. It should be noted that through the processing of the PMU measurements by a dynamic SE, the noise that is encompassed in the measurements can be filtered. At the same time, it is possible to detect and identify bad PMU measurements provided by a malfunctioned PMU. Thus, SE is more preferable compared to simply reading the raw PMU measurements.

The commonly used SE model is given by [8],

$$\mathbf{z} = \mathbf{h}(\mathbf{x}) + \mathbf{e}, \quad (4)$$

where, \mathbf{z} is the measurement vector; $\mathbf{h}(\mathbf{x})$ is the vector containing the equations that relates the measurements to the system states; \mathbf{x} is the state vector containing the power system states (i.e., bus voltage magnitudes and bus voltage angles); and \mathbf{e} is the Gaussian noise introduced in the measurements.

In order to have a unique estimation for the states, the power system should be observable by the given set of measurements. The PMU can provide both the voltage phasor of the bus that is

connected and all the current phasors of the branches emanating from the PMU bus (assuming enough current measurement channels). In order to express the current phasor measurements with a linear relation to the states of the power system, the voltage phasors should be transformed to rectangular form. Based on *Figure 3*, and assuming that a PMU is installed at bus s , the current phasor \bar{I}_s is related to the states of the power system as,

$$\bar{I}_s = \bar{V}_s(g_{sh} + jb_{sh}) + (\bar{V}_s - \bar{V}_r)(g_{sr} + jb_{sr}) \quad (5)$$

where \bar{V}_s and \bar{V}_r are the voltage phasors of buses s and r and can be expressed in rectangular form as,

$$\bar{V}_s = V_s \cos \theta_s + jV_s \sin \theta_s \quad (6)$$

$$\bar{V}_r = V_r \cos \theta_r + jV_r \sin \theta_r \quad (7)$$

The real and imaginary parts of the PMU current measurement in relation to the real and imaginary voltage phasor of bus s and bus r are calculated as,

$$I_{real}^{meas} = V_s \cos \theta_s (g_{sh} + g_{sr}) - V_s \sin \theta_s (b_{sh} + b_{sr}) + b_{sr} V_r \sin \theta_r - g_{sr} V_r \cos \theta_r \quad (8)$$

$$I_{imag}^{meas} = V_s \cos \theta_s (b_{sh} + b_{sr}) + V_s \sin \theta_s (g_{sh} + g_{sr}) - b_{sr} V_r \cos \theta_r - g_{sr} V_r \sin \theta_r . \quad (9)$$

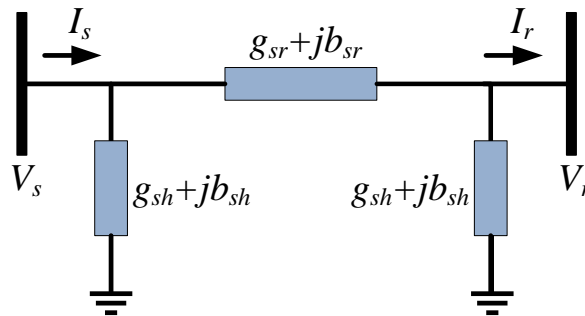


Figure 3: Transmission line parameter with a PMU at bus s

Therefore, using the model of the SE shown in (1), the PMU measurements are related to the power system states as,

$$\mathbf{z} = \mathbf{H}\mathbf{x} + \mathbf{e} = \begin{bmatrix} \mathbf{V}_r^{meas} \\ \mathbf{V}_i^{meas} \\ \mathbf{I}_r^{meas} \\ \mathbf{I}_i^{meas} \end{bmatrix} = \begin{bmatrix} \frac{\partial \mathbf{V}_r}{\partial \mathbf{V}_r} & \frac{\partial \mathbf{V}_r}{\partial \mathbf{V}_i} \\ \frac{\partial \mathbf{V}_i}{\partial \mathbf{V}_r} & \frac{\partial \mathbf{V}_i}{\partial \mathbf{V}_i} \\ \frac{\partial \mathbf{I}_r}{\partial \mathbf{V}_r} & \frac{\partial \mathbf{I}_r}{\partial \mathbf{V}_i} \\ \frac{\partial \mathbf{I}_i}{\partial \mathbf{V}_r} & \frac{\partial \mathbf{I}_i}{\partial \mathbf{V}_i} \end{bmatrix} \begin{bmatrix} \mathbf{V}_r \\ \mathbf{V}_i \end{bmatrix} + \mathbf{e}, \quad (10)$$

where,

\mathbf{z} containing the PMU measurements in rectangular form; \mathbf{H} is the Jacobian matrix that relates the measurements to the power system states; \mathbf{x} is the vector containing the power system states (in a dynamic SE there are the real and imaginary parts of the N buses voltage phasors); \mathbf{V}_r , \mathbf{V}_i , \mathbf{I}_r , \mathbf{I}_i are the

real and imaginary parts of the bus voltage phasors and the branch current phasors respectively when they are expressed in rectangular form.

Based on the WLS formulation, the state vector can be found by minimizing the function $J(\mathbf{x})$ as,

$$\text{Min } J(\mathbf{x}) = [\mathbf{z} - \mathbf{H}\mathbf{x}]\mathbf{R}^{-1}[\mathbf{z} - \mathbf{H}\mathbf{x}], \quad (11)$$

where, \mathbf{R} is the measurement error covariance matrix that is essentially used for weighting the PMU measurements according to their measurement accuracy.

Taking the derivative of $J(\mathbf{x})$ over \mathbf{x} and setting it to zero, the state vector can be found as,

$$\hat{\mathbf{x}} = (\mathbf{H}^T \mathbf{R}^{-1} \mathbf{H})^{-1} \mathbf{H}^T \mathbf{R}^{-1} \mathbf{z}. \quad (12)$$

According to (9), the states of the system can be estimated in a single shot without the need for any iterations, as in the contemporary SE scheme. This linearity allows the real time execution of the dynamic state estimator and the process of the PMU measurements as they arrive to the control center. This essentially enables the real time monitoring of the power system operating condition through the PMU measurements.

The linear state estimation above has been implemented and applied in the Cyprus power system after the implementation of the WAM system in Cyprus. In Figure 4, the estimated voltage magnitude and angle for Latsia substation is shown as it was provided by the linear state estimator. It is clearly indicated that the implemented PMU-based estimator can track quite accurately the fluctuations and the fast or slow transients of the system.

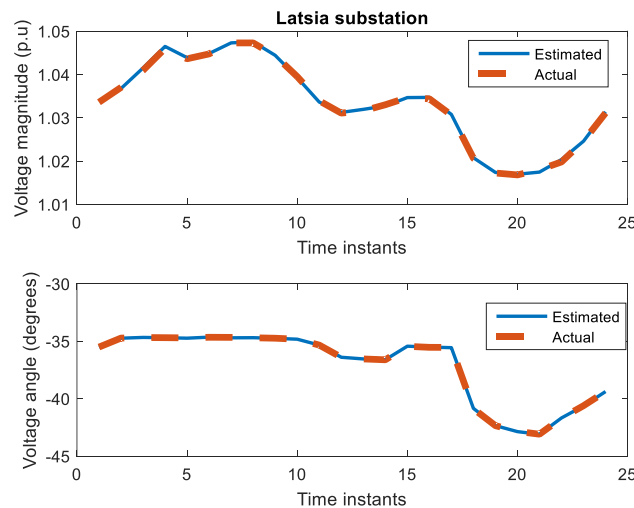


Figure 4: Voltage magnitude and angle of Latsia substation-Cyprus power system

1.3.2 Line parameter estimation

Accurate knowledge of transmission line parameters is crucial for various monitoring and control applications within the power system control center. Although these parameters are stored in control center databases, they are often assumed to be time-invariant. However, these databases may become outdated and contain erroneous information. Typically, the parameters are calculated using manufacturer data, which often ignores environmental factors (e.g., ambient temperature) that can affect their accuracy. Therefore, systematically refining these parameters can significantly enhance

the situational awareness of power system operators, while adaptive distance protection schemes can be implemented for more reliable protection of the system.

The presence of two PMUs at both ends of the line allows for real-time calculation of the line parameters using PMU data. Specifically, as illustrated in Figure 3, and assuming that the sending and receiving voltage and current phasors are available through PMUs, the series impedance and shunt susceptance can be determined as follows:

$$g_{sr} + jb_{sr} = \frac{\tilde{I}_s \tilde{V}_r + \tilde{V}_s \tilde{I}_r}{\tilde{V}_s^2 - \tilde{V}_r^2} = \frac{1}{R + jX} \quad (13)$$

$$g_{sh} + jb_{sh} = \frac{\tilde{I}_s - \tilde{I}_r}{\tilde{V}_s + \tilde{V}_r} \quad (14)$$

In the case of the Cyprus WAM, the transmission line parameters were calculated for the lines monitored by two PMUs. The reporting rate of the PMUs was 50 phasors per second, which corresponds to 180000 measurements per hour. Considering that the value of the parameters remains constant within one hour interval the average value of the parameters calculated in one hour (using the 180000 measurements) was used for representing the parameters' value of each hour.

The variation of the series resistance (Ω) and its deviation from nominal value (%) in different weather conditions for weekdays and weekends are shown in Figure 5 and Figure 6. The deviation of the calculated series resistances from the nominal during the day for these cases ranges from 9% to 25%. In addition, during the summer, the value of the series resistance is higher in comparison to the winter periods. This is also verified by the physics behind the resistance since the resistance varies linearly with respect to the operating temperature.

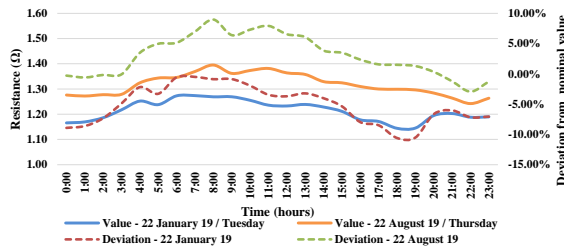


Figure 5: Comparison and deviation from nominal value of series resistance between different weather condition for weekdays

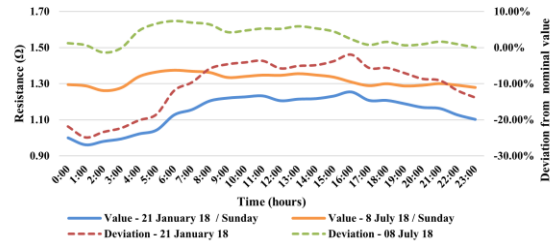


Figure 6: Comparison and deviation from nominal value of series resistance between different weather condition for weekends

Regarding the series reactance, Figure 7 and Figure 8 show the variation of the series reactance (Ω) and its deviation from nominal value (%) for different weather conditions for weekdays and weekends, respectively. The deviation of the calculated series reactance from the nominal value during the day, for these cases, ranges between 4% to 6.5%. The series reactance is a bit larger in summer than in winter, however according to the conclusions of this work the series reactance is affected by the loading conditions rather than the temperature.

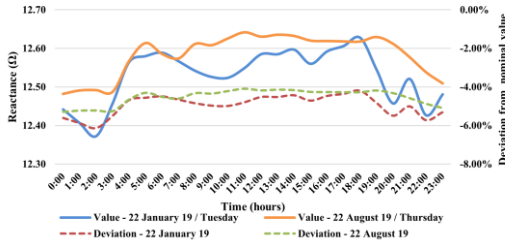


Figure 7: Comparison and deviation from nominal value of series reactance between different weather condition for weekdays

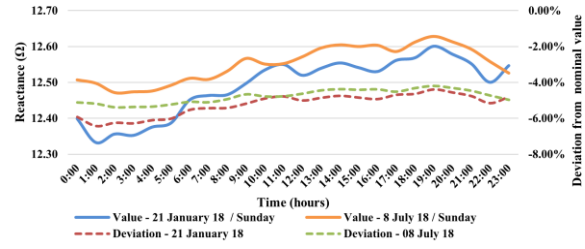


Figure 8: Comparison and deviation from nominal value of series reactance between different weather condition for weekends

1.3.3 Inertia estimation

The increasing penetration of Renewable Energy Sources (RESs) presents significant challenges to the secure and stable operation of power systems. Traditionally, system inertia has relied on the physical inertia of the rotating mass of conventional synchronous generators. However, as these conventional plants are replaced by non-rotating RESs, such as photovoltaics, system inertia decreases, thereby threatening system stability. Even with rotating RESs like wind power systems, the use of power electronics converters decouples the physical inertia of the turbines, negating their contribution to overall system inertia. Consequently, the green transition of power systems leads to low-inertia grids, where system frequency becomes highly sensitive to generation-load imbalances. Rapid frequency changes, characterized by a higher rate of change of frequency (RoCoF), can trigger protection systems, potentially causing system separation, loss of generation, and loss of load.

In this context, real-time information about system inertia becomes critically important in power systems with high renewable energy penetration. This need can be met through the use of PMU measurements provided by WAM systems. The dynamics between power and frequency following a power mismatch can be described by the swing equation. For a single synchronous generator, the swing equation is given by,

$$2H\Delta\dot{f} = P_m - P_e - D\Delta f \quad (15)$$

where Δf is the rotor electrical frequency deviation from the nominal value (p.u.); P_m is the mechanical power (p.u.); P_e is the electrical power (p.u.); D is the damping factor; and H is the inertia constant (sec). The closed-loop equivalent transfer function $G(s)$, which corresponds to the frequency deviation from the nominal frequency (Δf) according to the active power deviation from the generator's set-point reference (ΔP) is given by,

$$G(s) = \frac{-R(1 + sT_G)(1 + sT_C)(1 + sT_R)}{(2Hs + D)(1 + sT_G)(1 + sT_C)(1 + sT_R)R + sF_H T_R + 1} \quad (16)$$

The equivalent transfer function of (16) can be simplified to a lower order model, as the smaller time constants can be neglected. The most significant time constants (e.g., T_R , H , $1/R$) dominate the

response and the low-order equivalent model and thus, $G(s)$ can be approximated by an n -order transfer function,

$$G(s) = \frac{\Delta f}{\Delta P} = \frac{b_{n-1}s^{n-1} + \dots + b_1s + b_0}{s^n + a_{n-1}s^{n-1} + \dots + a_1s + a_0} \quad (17)$$

The order of the transfer function has to be large enough to capture the main dynamics of the system and the inertia constant can be extracted from the term b_{n-1} of (17), as $b_{n-1} = 1/(2H)$ when a_n is equal to one [9]. The equivalent transfer function as given of (17) can be re-written in the form of a differential equation as,

$$\Delta f^{(n)} + a_{n-1}\Delta f^{(n-1)} + \dots + a_1\dot{\Delta f} + a_0\Delta f = b_{n-1}\Delta P^{(n-1)} + \dots + b_1\dot{\Delta P} + b_0\Delta P \quad (18)$$

where the order n of the transfer function corresponds also to the order of the differential equation and $\Delta f^{(n)}$ is the n^{th} -order time derivative of the frequency deviation Δf . In a similar manner the $n-1$ time derivative $\Delta P^{(n-1)}$ of the power deviation is defined. The differential equation of (18) can be rearranged in the following form.

$$\Delta f^{(n)} = -a_{n-1}\Delta f^{(n-1)} - \dots - a_1\dot{\Delta f} - a_0\Delta f + b_{n-1}\Delta P^{(n-1)} + \dots + b_1\dot{\Delta P} + b_0\Delta P \quad (19)$$

In this form, the parameter b_{n-1} is related only to the inertia constant and does not include other model parameters.

The frequency (Δf) and power (ΔP) signals that are obtained by the WAM system can be used in the LS method for estimating generator inertia. Considering a 2nd-order model for a single generator, (19) can be written as,

$$\dot{\Delta f} = -a_1^s\dot{\Delta f} - a_0^s\Delta f + b_1^s\dot{\Delta P} + b_0^s\Delta P \quad (20)$$

where subscripts s describes the parameters of the second order models. The parameter \hat{b}_1^s can be identified by solving the LS problem below,

$$\text{minimize } \sum_{i=1}^I (y_{2,i} - \hat{y}_{2,i})^2 \quad (21)$$

$$\text{s.t. } y_{2,i} = -a_1^s y_{1,i} - a_0^s y_{0,i} + b_1^s u_{1,i} + b_0^s u_{0,i} \quad \forall i \in I \quad (22)$$

The inertia estimation was applied to the Cyprus power system for estimating the inertia provided by the generating stations of the Cyprus power system. Indicatively, the maximum and average estimation error in a time window of 1 hour is shown in Table 2.

Table 2: Inertia estimation error for a generation substation in Cyprus

True inertia value (sec)	Average error (%)	Maximum error (%)
5.25	2.03	5.79

1.3.4 Contribution to development of low carbon technologies, sustainability and circularity

Wide Area Monitoring Systems (WAMS) significantly contribute to the development of low carbon technologies, sustainability, and circularity in the power sector. By providing real-time data on grid conditions, WAMS facilitate the integration of renewable energy sources, improve grid efficiency, and support decentralized energy resources. This optimization reduces reliance on fossil fuels, lowers carbon emissions, and enhances grid stability and flexibility. Additionally, WAMS enable predictive maintenance, which extends the lifespan of grid infrastructure, reduces waste, and supports a circular economy.

1.3.5 Highlight on application in industry

This training material is built upon the valuable lessons learned from implementing a Wide Area Monitoring (WAM) system in the Cyprus power system, making it highly relevant and applicable to the industry. The training aims to motivate power system operators to engage in the implementation of WAM systems by demonstrating their numerous advantages. By sharing practical insights and experiences from the Cyprus power system, the training material provides a clear understanding of the benefits and challenges of WAM systems in real-world scenarios.

Additionally, the training is also designed for highlighting the application of three WAM-based schemes: state estimation, line parameter estimation, and inertia estimation in the real field. These schemes have been validated and tested using measurements from PMUs in the Cypriot WAM system. The results presented in the training highlight the practical applicability of these methodologies and techniques, emphasizing the importance of an operational WAM system in modern power systems. By showcasing these real-world applications, the training clearly points out the critical role of WAM systems in enhancing grid reliability, efficiency, and overall performance.

1.3.6 Contribution to development of skills and competences

The training material created in the context of the TRANSIT project on the implementation of WAM systems significantly enhances the skills and competencies of employees in the industry and other stakeholders. It provides in-depth technical knowledge on the design, deployment, and operation of WAM systems, covering essential aspects such as data acquisition, communication protocols, and system integration. This technical proficiency is vital for ensuring the reliability and efficiency of grid operations. Additionally, the information for WAM-based applications that were provided in this training enhances data analysis and interpretation of the operators and equips them to make informed decisions and address grid inefficiencies, improving in this way the overall operational effectiveness.

Moreover, the industry best practices, standards, and regulatory requirements that are summarized in this training material, ensuring that stakeholders implement WAMS in compliance with the latest developments. In addition, the training of the TRANSIT project in WAMs promotes collaboration across various fields including telecommunication, data analytics, power systems, and ICT. In this

sense, the training ensures effective collaboration among different industrial stakeholders that ultimately leads to improved grid performance, sustainability, and continuous innovation in the power sector.

1.4 References

- [1] A. G. Phadke and T. S. Thorp, *Synchronized Phasor Measurements and Their Applications*. New York: Springer, 2008.
- [2] "IEEE Standard for synchrophasors for power systems," IEEE Standard 1344-1995, 1995.
- [3] "IEEE Standard for Synchrophasors for Power Systems," IEEE Std C37.118-2005, 2005.
- [4] "IEEE standard for synchrophasors for power systems," IEEE Std C37.118.1-2011, 2011.
- [5] IEEE Standard for Synchrophasor Measurements for Power Systems -- Amendment 1: Modification of Selected Performance Requirements," in IEEE Std C37.118.1a-2014
- [6] M. Kezunovic, S. Meliopoulos, V. Venkatasubramanian, and V. Vittal, *Application of Time-Synchronized Measurements in Power System Transmission Networks.*: Springer International Publishing, 2014.
- [7] M. Asprou, E. Kyriakides and S. Chakrabarti, "The use of a PMU-based state estimator for tracking power system dynamics," 2014 IEEE PES General Meeting, National Harbor, MD, USA, 2014, pp. 1-5.
- [8] F. C. Swebpe and J. Wildes, "Power system static state estimation, Part I: Exact model," IEEE Transactions on Power Apparatus, vol. 89, pp. 120-125, Jan. 1970.
- [9] K. Tuttelberg, J. Kilter, D. Wilson, and K. Uhlen, "Estimation of power system inertia from ambient wide area measurements," IEEE Trans. Power Syst., vol. 33, no. 6, pp. 7249–7257, 2018.